American Mineralogist, Volume 58, pages 998–1008, 1973

Two-Phase Data for the Join Monticellite ($CaMgSiO_4$)-Forsterite (Mg_2SiO_4): Experimental Results and Numerical Analysis

RICHARD D. WARNER[1]

*Planetology Branch, Goddard Space Flight Center,
Greenbelt, Maryland 20771*

WILLIAM C. LUTH

*Department of Geology, Stanford University,
Stanford, California 94305*

Abstract

Subsolidus equilibria along the $CaMgSiO_4$–Mg_2SiO_4 olivine join are governed by partial immiscibility between the end-member phases. The solvi bounding the two-phase region are determined over the temperature range 800–1300°C at 2, 5, and 10 kbar. Within the limits of experimental error, the two-phase data are symmetric with respect to composition. Numerical analysis of the experimental data in terms of a one-constant Margules equation (Thompson, 1967) yields the following relationship for the mixing parameter of the Gibbs Free Energy Function:

$$W_G(\text{cal/mole}) = 20{,}338 \pm 2355 - 13{,}560 \pm 3412 \times T(^\circ\text{K})/1000 + 3627 \pm 1228 \times (T/1000)^2 - 355.4 \pm 87.5 \times P(\text{kbar}) + 308.7 \pm 65.4 \times P(T/1000), \text{S.D.} = 297.4$$

Temperature-composition sections of the two-phase region calculated from this equation are in good agreement with the experimental data. The results imply that the maximum amount of $CaMgSiO_4$ which may be dissolved in forsteritic olivine is less than 5 mole percent under physico-chemical conditions likely to exist in natural systems.

Introduction

In terms of the common rock-forming silicates, Ca ⇆ Mg substitution may be an important petrogenetic indicator. Because of the disparity in cation size [6-coördinated ionic radii 1.00 Å and 0.72 Å, respectively (Shannon and Prewitt, 1969)], systems involving Ca ⇆ Mg substitution tend to exhibit only limited miscibility between the crystalline end-member phases. For such systems, experimental data outlining the limits of miscibility as a function of temperature and pressure yield information of potential applicability to geothermometry and geobarometry. Through the application of a suitable solution model, such data may be used also to calculate useful thermodynamic quantities for the crystalline solutions involved (*e.g.*, Thompson, 1967; Thompson and Waldbaum, 1969; Saxena, 1972).

The monticellite ($CaMgSiO_4$)–forsterite (Mg_2SiO_4) system has been chosen for study because the two end-member phases display similar crystal structures (both belong to space group *Pbnm*), and because no polymorphic changes occur within the stability range of the monticellite-forsterite two-phase coexistence. The primary objectives of this study are to map the boundary of the monticellite-forsterite two-phase region as a function of temperature at several pressures (2, 5, and 10 kbar were chosen), and to derive an equation of state and activity-composition relations for the olivine crystalline solutions. The results may then be used to correlate the Ca content of forsteritic olivine with P, T conditions of crystallization.

Previous Work

In their study of solidus-liquidus relations in the system CaO–MgO–SiO_2 at 1 atm, Ferguson and Merwin (1919) demonstrated the existence of limited (up to about ten wt percent) crystalline solution of Mg_2SiO_4 in monticellite. They also reported that pure monticellite was unstable in the temperature range investigated. Ricker and Osborn (1954) further in-

---

[1] Presently a National Academy of Sciences Resident Research Associate at Goddard Space Flight Center.

vestigated phase equilibrium relationships along the join $CaMgSiO_4$–Mg_2SiO_4 at 1 atm. At near-liquidus temperatures, crystalline solution was found to extend approximately 30 wt percent from either end-member. The extent of crystalline solution was shown to decrease (*i.e.*, the monticellite-forsterite two-phase region widens) rapidly with decreasing temperature. More recent 1 atm data for this system (Biggar and O'Hara, 1969) suggest that the extent of crystalline solution is less than that reported by Ricker and Osborn (1954). According to Biggar and O'Hara (1969), the estimated range of stable crystalline solutions is 75 to 92 mole percent monticellite and 81 to 100 mole percent forsterite, respectively, at 1490°C. In addition, Biggar and O'Hara (1969) confirmed that $CaMgSiO_4$ is unstable at atmospheric pressure. Yang (1973) studied the monticellite-forsterite solvi between 1440°C and 1496°C at 1 atm by means of electron microprobe analysis of coexisting monticellite and forsterite crystallized from melts with compositions off the $CaMgSiO_4$–Mg_2SiO_4 join. His determinations indicate that the amount of $CaMgSiO_4$ which may be dissolved in forsterite varies from 13.5–14.5 wt percent at 1440°C to 17.2–18.7 at 1496°C, whereas the amount of Mg_2SiO_4 in monticellite varies from 16.2–18.0 wt percent at 1440°C to 27.2 to 28.7 at 1496°C.

Experimental studies by Kushiro and Yoder (1964) and Yoder (1968) have shown that at high pressures monticellite breaks down to the assemblage merwinite ($Ca_3MgSi_2O_8$) + a forsterite crystalline solution. The *P-T* curve for this reaction originates from an invariant point at 1095°C and 10.6 kbar and has a large negative dT/dP slope (about −160°C/kbar) according to Yoder (1968).

Experimental Results[1]

Results of Synthesis Experiments

Synthesis of single-phase materials (experimental apparatus and procedure described in Appendix) along the join $CaMgSiO_4$–Mg_2SiO_4 (Table 2) were carried out for the purpose of selecting an X-ray peak or peaks whose variation with composition could be used for rapid determination of compositions of coexisting olivines. Trace amounts of periclase, never in excess of 1–2 percent by volume, were detected in a number of 1 atm runs; no periclase was observed in the products of hydrothermal syntheses. Presence of periclase in the 1 atm runs is considered to reflect incomplete reaction. All attempts to synthesize the monticellite end-member were unsuccessful. Instead, this composition always crystallized to a monticellite solution containing several wt percent Mg_2SiO_4 plus minor merwinite ($Ca_3MgSi_2O_8$), the latter phase exceeding 10 percent by volume in runs at 1450°C and 1 atm. This finding corroborates earlier reports on the instability of $CaMgSiO_4$ (Ferguson and Merwin, 1919; Biggar and O'Hara, 1969).

The variation with N_{fo} of $2\theta_{131}$ was selected for determining olivine compositions. The 131 peak was selected because it is one of the strongest olivine peaks, varies linearly with composition, and is close to both the 220 and 311 peaks of the spinel internal standard. The linear equations relating this parameter to composition are given by

$$N_{fo} = -18.115 + 0.539(2\theta^{A}_{131}) \qquad (1)$$

$$N_{fo} = -20.360 + 0.597(2\theta^{B}_{131}) \qquad (2)$$

where A and B refer to the $CaMgSiO_4$- and Mg_2SiO_4-rich phases, respectively. Determinations obtained through the use of these equations are believed accurate to within ±0.015 N_{fo}.

Results of least-squares cell refinements of synthetic Ca/Mg olivines are furnished in Table 3 and plotted in Figure 1. The chief contribution to the change in unit cell volume comes from variation of the *b* cell edge; the *c* cell edge is only moderately affected by Ca ⇆ Mg substitution, while the *a* cell edge is virtually unaffected. With reference to the end-member phases, the series of crystalline solutions

TABLE 1. Explanation of Symbols Used in Text

Component designations

mo = $CaMgSiO_4$
fo = Mg_2SiO_4
$mo_x fo_y$ = composition of phase or mixture (in weight percent)

Phase designations

Mo = monticellite
Fo = forsterite
Me = merwinite
P = periclase
L = silicate liquid, generally containing dissolved water
V = hydrous vapor, containing dissolved silicate components
ss = subscript refers to solid solution phases

Thermochemical designations

N_{fo} = mole fraction Mg_2SiO_4
α = dimensionless parameter denoting number of crystal substitution sites
W_G = Margules parameter of molar Gibbs function
ex = subscript refers to thermodynamic excess function
mix = subscript refers to thermodynamic mixing function
a_i = relative activity of component i

---

[1] For an explanation of the symbols used in the text, see Table 1.

TABLE 2. Olivine Synthesis Data

Starting material composition	Wt.% H_2O	P(bars)	T(°C)	t(hrs)	Results
		a) 1 bar data			
mo_{100}			1440	21	$Mo_{ss}+Me$
$mo_{95}fo_5$			"	"	$*Mo_{ss}+\underline{Me}$
$mo_{90}fo_{10}$			"	"	$*Mo_{ss}$
$mo_{85}fo_{15}$			"	"	$*Mo_{ss}$
$mo_{30}fo_{70}$			1440	23	$Fo_{ss}+\underline{Mo}_{ss}$
$mo_{25}fo_{75}$			"	"	$Fo_{ss}+\underline{Mo}_{ss}$
$mo_{20}fo_{80}$			"	"	$Fo_{ss}+\underline{Mo}_{ss}$
mo_{100}			1455	31	$Mo_{ss}+Me$
$mo_{95}fo_5$			"	"	$Mo_{ss}+\underline{Me}$
$mo_{90}fo_{10}$			"	"	Mo_{ss}
$mo_{85}fo_{15}$			1450	26	Mo_{ss}
$mo_{80}fo_{20}$			"	"	$*Mo_{ss}$
$mo_{75}fo_{25}$			"	"	$Mo_{ss}+\underline{Fo}_{ss}$
$mo_{70}fo_{30}$			1450	38	$Mo_{ss}+Fo_{ss}$
$mo_{15}fo_{85}$			1450	16	$*Fo_{ss}+\underline{P}'$
$mo_{10}fo_{90}$			"	"	$*Fo_{ss}+\underline{P}'$
mo_5fo_{95}			"	"	$*Fo_{ss}+\underline{P}'$
fo_{100}			"	"	$*Fo+\underline{P}'+\underline{SG}'$
$mo_{30}fo_{70}$			1450	170	$Fo_{ss}+Mo_{ss}$
$mo_{25}fo_{75}$			"	"	$Fo_{ss}+Mo_{ss}$
$mo_{20}fo_{80}$			"	"	$*Fo_{ss}+\underline{Mo}_{ss}$
$mo_{15}fo_{85}$			"	"	$*Fo_{ss}$
		b) hydrothermal data			
fo_{100}	19	500	890	120	$*Fo+\underline{P}'+\underline{SG}'+V$
$mo_{10}fo_{90}$	15	1000	1240	14	$*Fo_{ss}+V$
$mo_{95}fo_5$	16	2000	1150	50	$*Mo_{ss}+V$
$mo_{90}fo_{10}$	18	"	"	"	$Mo_{ss}+\underline{Fo}_{ss}+V$
$mo_{85}fo_{15}$	17	"	"	"	$Mo_{ss}+Fo_{ss}+V$
$mo_{15}fo_{85}$	19	"	"	"	$Fo_{ss}+Mo_{ss}+V$
$mo_{10}fo_{90}$	20	"	"	"	$Fo_{ss}+\underline{Mo}_{ss}+V$
mo_5fo_{95}	19	"	"	"	$*Fo_{ss}+V$
mo_{100}	18	2000	1250	72	$Mo_{ss}+\underline{L}?+V$
mo_{100}	8.5	5000	850	330	$Mo_{ss}+\underline{Me}+V$
mo_{100}	16	5600	1000	120	$*Mo_{ss}+\underline{Me}+V$
mo_5fo_{95}	12.5	10,000	1150	19	$*Fo_{ss}+V$
fo_{100}	12	"	"	"	$*Fo+V$

Abbreviations: SG = silica glass (unreacted); other phase and component designations as in Table 1
* = least squares cell refinement performed on olivine (Table 3)
' = presence of phase thought to be metastable
_ = amount of phase present estimated at less than 5 volume percent

TABLE 3. Unit Cell Dimensions of Synthetic Olivines

N_{fo}	a(Å)	b(Å)	c(Å)	V(Å^3)	n/m
0.010*	4.8209(5)	11.0911(9)	6.3726(6)	340.74(4)	25/29
0.055*	4.8201(7)	11.0530(10)	6.3552(7)	338.59(5)	20/26
0.065	4.8202(8)	11.0506(19)	6.3519(12)	338.34(7)	20/24
0.110	4.8180(6)	11.0074(9)	6.3327(6)	335.84(4)	26/32
0.164	4.8152(6)	10.9599(15)	6.3092(9)	332.96(6)	18/24
0.218	4.8139(9)	10.9131(14)	6.2921(11)	330.56(7)	17/22
0.820#	4.7694(4)	10.3180(11)	6.0353(7)	297.00(4)	34/36
0.863	4.7664(5)	10.2926(13)	6.0230(7)	295.48(4)	32/35
0.909	4.7606(4)	10.2499(10)	6.0023(6)	292.89(3)	27/27
"	4.7596(5)	10.2463(16)	6.0027(10)	292.74(6)	27/27
0.955	4.7585(5)	10.2248(11)	5.9933(6)	291.61(4)	29/30
"	4.7581(3)	10.2230(7)	5.9929(4)	291.51(3)	33/34
"	4.7575(3)	10.2144(10)	5.9900(5)	291.08(3)	38/41
1.000	4.7537(6)	10.1980(11)	5.9811(6)	289.96(4)	27/28
"	4.7555(6)	10.1996(10)	5.9827(6)	290.18(4)	24/24
"	4.7549(3)	10.1976(11)	5.9824(6)	290.08(4)	35/38

n/m = number of lines used in refinement/number of input diffraction lines
Numbers in () represent errors in final figures at the unit weight standard error level
*Approximate N_{fo} based on optical estimate of amount of merwinite (Me) in sample product
\#Approximate N_{fo} based on estimate of amount of Mo_{ss} in sample product

extending from $CaMgSiO_4$ displays no volume of mixing, whereas the forsterite-rich solutions show a slight negative volume of mixing.

Results of Two-Phase Determinations

The solvi bounding the monticellite-forsterite two-phase region were determined by homogenization experiments at 50°C intervals over the temperature range 800°–1300°C. Isobars at 2, 5, and 10 kbar were mapped out in this manner. All experiments were made under hydrothermal conditions in order to expedite the reaction rate. (At temperatures above the vapor-saturated solidus, it was found necessary to load only a few wt percent water in order to insure that the two-olivine assemblage, here Mo_{ss} + Fo_{ss} + L, was obtained.) X-ray exposures with a focusing camera were taken of the run products, and olivine compositions were obtained by measuring $2\theta_{131}$ (Equations 1 and 2).

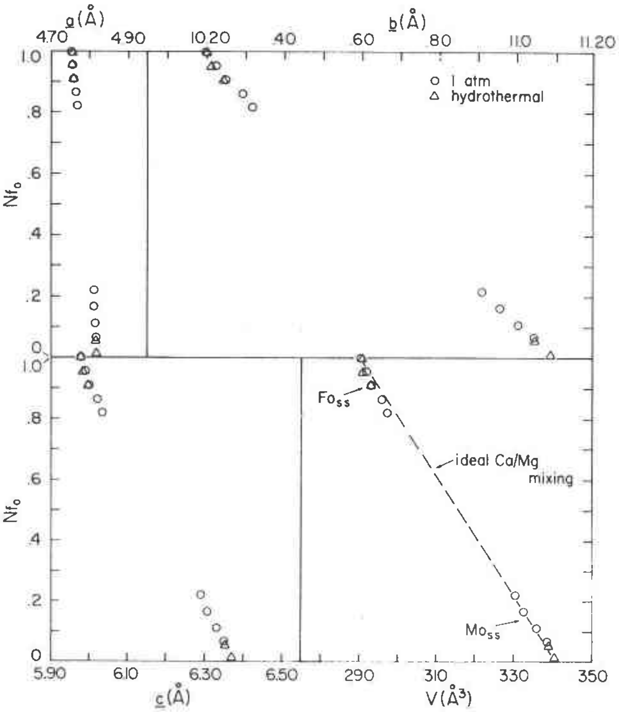

FIG. 1. The observed relationship between N_{fo} and the *a*, *b*, and *c* cell edges and unit cell volume for synthetic monticellite and forsterite crystalline solutions. Data from Table 3. The dashed line indicates ideal Ca/Mg mixing as defined by the two end-members.

The experimental results are presented in Table 4. Where two or more samples were run simultaneously, agreement to within 0.01 N_{fo} was observed. Reproducibility of the results was tested by a number of runs duplicating conditions of pressure and temperature of a previous determination but differing in duration. Again, agreement to within 0.01 N_{fo} was observed. The solvi were reversed at 900° and 1200°C at 2 kbar by unmixing a two-phase assemblage previously heated at 1450°C and 1 atm (Table 4 (d)). These findings strongly imply the general attainment of equilibrium throughout this study.

At 10 kbar the two phase region apparently widens at temperatures above 1200°C [Table 4(f), Figure 2(b)]. In general, discontinuous changes in slope along a solvus result from phase reactions. In this case, it is possible to relate the observed behavior to the reaction $Mo_{ss} = Me + Fo_{ss}$. This reaction (Kushiro and Yoder, 1964) represents the maximum upper thermal stability of Mo_{ss} at a given pressure, and the monticellite participating in this reaction will be of some unique composition. On the basis of previous studies (Ferguson and Merwin, 1919; Biggar and O'Hara, 1969) it is probable that the composition of Mo_{ss} that is in univariant equilibrium with Me and Fo_{ss} is enriched in Mg_2SiO_4 relative to stoi-

TABLE. 4. Monticellite-Forsterite Two-Phase Data

T(°C)	t(hrs)	$2\theta^A_{131}$	$2\theta^B_{131}$	N_{2A}	N_{2B}	r
a) 1 atm data						
1450	38	34.034	35.425	0.228	0.789	0.017
1450	170	34.043	35.433	0.234	0.794	0.028
b) 1 kb data						
1240	14	33.825	35.612	0.117	0.900	0.017
1280	21	33.856	35.593	0.133	0.889	0.022
c) 2 kb data (homogenization)						
800	229	33.639	35.762	0.016	0.990	0.006
"	"	33.633	35.752	0.013	0.984	-0.003
"	"	33.636	35.764	0.014	0.991	0.005
850	212	33.643	35.761	0.018	0.989	0.007
"	"	33.641	35.754	0.017	0.985	0.002
900	157	33.644	35.754	0.019	0.985	0.004
"	"	33.650	35.758	0.022	0.988	0.010
950	158	33.652	35.738	0.023	0.976	-0.001
"	"	33.660	35.744	0.028	0.979	0.007
1000	110	33.666	35.718	0.030	0.964	-0.006
"	"	33.680	35.725	0.038	0.968	0.006
"	"	33.674	35.723	0.035	0.967	0.002
1050	192	33.678	35.709	0.037	0.958	-0.005
"	"	33.685	35.711	0.041	0.959	0.000
1050	70	33.692	35.723	0.045	0.967	0.012
1100	117	33.710	35.686	0.054	0.945	-0.001
"	"	33.711	35.679	0.055	0.940	-0.005
"	"	33.704	35.688	0.052	0.946	-0.002
1100	65	33.711	35.683	0.055	0.943	-0.002
1150	50	33.727	35.659	0.064	0.928	-0.008
1150	120	33.736	35.671	0.069	0.936	0.005
"	"	33.733	35.668	0.067	0.934	0.001
1150	86	33.725	35.657	0.063	0.927	-0.010
1200	45	33.787	35.627	0.096	0.909	0.005
"	"	33.789	35.630	0.097	0.911	0.008
1235	20	33.797	35.604	0.102	0.896	-0.002
1300	17	33.856	35.616	0.133	0.903	0.036
d) *2 kb data (unmixing)						
900	167	33.654	35.734	0.025	0.973	-0.002
"	"	33.660	35.734	0.028	0.973	0.001
1200	17	33.762	35.623	0.083	0.907	-0.010
"	"	33.772	35.632	0.088	0.912	0.000
e) 5 kb data						
800	216	33.624	35.756	0.008	0.986	-0.006
850	330	33.644	35.756	0.019	0.986	0.005
"	"	33.638	35.755	0.016	0.986	0.002
900	118	33.641	35.749	0.017	0.982	-0.001
950	117	33.650	35.721	0.022	0.965	-0.013
1000	91	33.669	35.704	0.032	0.955	-0.013
1050	65	33.690	35.706	0.044	0.956	0.000
1100	66	33.711	35.691	0.055	0.948	0.003
1155	36	33.752	35.675	0.077	0.938	0.015
"	"	33.758	35.676	0.080	0.938	0.018
1200	32	33.757	35.666	0.080	0.932	0.012
1240	22	33.759	35.662	0.081	0.930	0.011
"	"	33.758	35.685	0.080	0.944	0.024
1300	18	33.781	35.656	0.093	0.927	0.020
f) 10 kb data						
800	324	33.633	35.761	0.013	0.989	0.002
"	"	33.626	35.757	0.009	0.987	-0.004
850	218	33.636	35.755	0.014	0.986	0.000
"	"	33.632	35.762	0.012	0.990	0.002
900	139	33.637	35.740	0.015	0.977	-0.008
"	"	33.637	35.746	0.015	0.980	-0.005
950	119	33.651	35.734	0.023	0.973	-0.004
1000	70	33.666	35.717	0.030	0.963	-0.007
1050	20	33.685	35.680	0.041	0.941	-0.018
1100	90	33.725	35.679	0.063	0.940	0.003
"	"	33.730	35.705	0.065	0.956	0.021
1230	19	33.743	35.680	0.073	0.941	0.014
1245	21	33.739	35.684	0.070	0.943	0.013
"	"	33.736	35.685	0.069	0.944	0.013
1300	16	33.706	35.697	0.052	0.951	0.003

$2\theta^A_{131}$ = measured value of $2\theta_{131}$ (Cu K_α radiation) for monticellite crystalline solution

$2\theta^B_{131}$ = measured value of $2\theta_{131}$ (Cu K_α radiation) for forsterite crystalline solution

N_{2A} = mole fraction Mg_2SiO_4 in monticellite crystalline solution

N_{2B} = mole fraction Mg_2SiO_4 in forsterite crystalline solution

$r = N_{2A} + N_{2B} - 1$

*Starting material used: $Mo_{ss}(N_{fo} = 0.222) + Fo_{ss}(N_{fo} = 0.789)$
$Mo_{ss}(N_{fo} = 0.232) + Fo_{ss}(N_{fo} = 0.794)$

chiometric monticellite, near $mo_{93}fo_7$ at 10 kbar as shown schematically in Figure 3. Yoder (1968) located this reaction at 1200°C, 10 kbar, although we did not find any evidence of this reaction at temperatures to 1300°C at 10 kbar. In Figure 3 this reaction is assumed to take place at some temperature greater than 1300°C. This explanation of the reversal in slope of the solvus limb is not wholly satisfactory in that it would generally be expected that the slope of the Fo_{ss} limb of the solvus would decrease, not increase as shown in Figure 2(b), as the univariant reaction is approached from the lower temperature regime. The close correlation of this solubility reversal with beginning of melting under hydrous conditions (approximately 1050°C at 10 kbar, Warner, 1973) suggests another possible explanation. The solidus reaction along the olivine join at this pressure is $Mo_{ss} + V = Fo_{ss} + L$ (Warner, 1973). At temperatures above this reaction forsterite crystalline solutions are present in three different phase assemblages: $Fo_{ss} + Mo_{ss} + L$; $Fo_{ss} + L$; and $Fo_{ss} + L + V$. This sequence of phase assemblages corresponds to an increase in H_2O content, and a decreasing monticellite solubility in the forsterite crystalline solutions for a given bulk composition on the olivine join. For this reason, the experiments (Table 4f) were conducted with H_2O content low enough to ensure that the bulk composition was in the composition region appropriate for the maximum solubility of monticellite in forsterite, $Mo_{ss} + Fo_{ss} + L$. Unfortunately, quench liquid products tend to obscure the equilibrium phase assemblage, so that appearance of monticellite in the X-ray patterns of the experimental products did not necessarily imply equilibrium coexistence under the pressure-temperature conditions of the experiment. Therefore, the results of X-ray analysis were supplemented by careful microscopic examination, and only those experimental products demonstrably in the $Mo_{ss} + Fo_{ss} + L$ field are included in the monticellite-forsterite two-phase data given in Table 4. Consequently, the reversal in solubility exhibited by the forsterite solvus limb is not satisfactorily explained by the univariant reaction $Mo_{ss} + V = Fo_{ss} + L$, as related to phase assemblages other than $Mo_{ss} + Fo_{ss} + L$.

An alternative explanation would involve metastability of either or both monticellite and forsterite at the higher temperatures. This explanation does not seem valid in view of the fact that the experiments at 1, 2, and 5 kbar at temperatures greater than 1200°C did not show the reversal in slope of the forsterite solvus limb (Table 4). It should be clear from the preceding discussion that we do not have a satisfactory explanation for the maximum in monti-

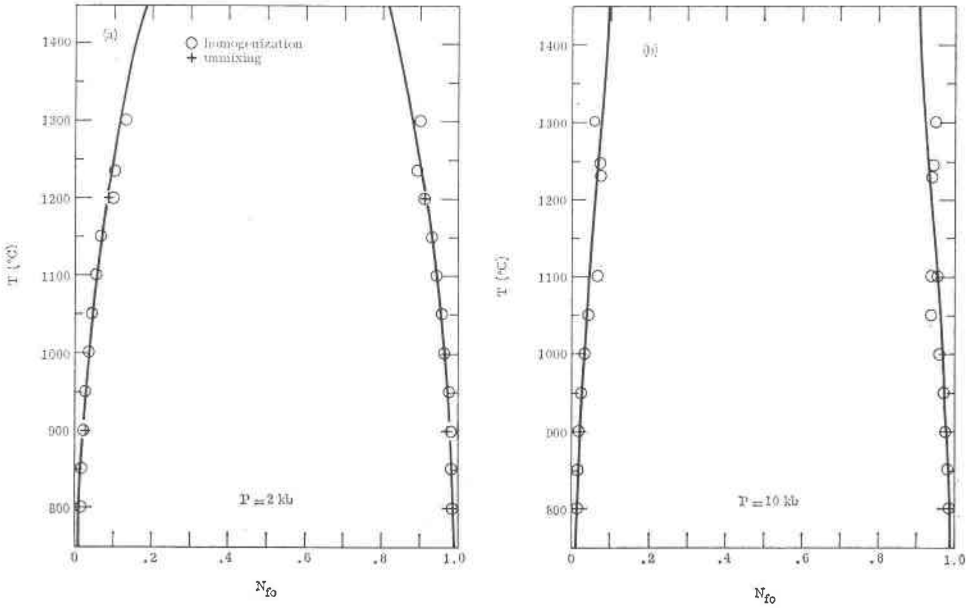

FIG. 2. Isobaric temperature-composition sections of the monticellite-fosterite two-phase region. The open circles indicate experimental determinations of the compositions of coexisting two-phase pairs (Table 4). The solid curves represent boundaries for the two-phase region calculated according to methods outlined in the text.

cellite solubility in the forsterite crystalline solutions shown by the data at 10 kbar. This feature is accepted as real, and the data at high temperatures are included in the following analysis of the two-phase data.

Numerical Analysis of Two-phase Data

Method of Treatment of Data

The two-phase data given in Table 4 permit derivation of an equation of state for the monticellite-forsterite olivine series. The method of analysis employed in this study involves the application of an abridged Margules-type expansion. The theoretical and analytic basis for this approach was discussed at some length by Thompson (1967) and thus need not be developed here. It is important to note that the theory is closely tied to the assumption that the laws of ideally dilute solutions are obeyed—that is, Henry's Law applies for the solute crystalline species, and Raoult's Law applies for the solvent crystalline species.

In treating the monticellite-forsterite crystalline series, some knowledge of the olivine crystal structure is required in order to assess the number of substitution sites which take part in the Ca/Mg mixing. Since in monticellite Ca is ordered into the $M(2)$ site and Mg into $M(1)$ (Onken, 1965), and since in forsterite the $M(2)$ site is larger than $M(1)$ (Birle *et al,* 1968), it seems reasonable to conclude that for the monticellite-forsterite crystalline series Ca/Mg mixing occurs solely at $M(2)$, and that $M(1)$ is filled by Mg. This is probably a valid assumption for $CaMgSiO_4$-rich compositions, but is open to some question for compositions close to Mg_2SiO_4. So that we may keep our treatment as simple as possible, we shall proceed on the basis of single-site substitution—that is, the partially miscible series is described by the formula $(Ca,Mg)MgSiO_4$. The value of the dimensionless parameter α, which denotes the number of crystal substitution sites (Thompson, p. 342, 1967), is thus taken as unity.

Inspection of the experimental data (Table 4) reveals that the two-phase region is approximately symmetric. The values for the compositional parameter r are very small and exhibit no consistent tendency to be either positive (asymmetric toward Mg_2SiO_4) or negative (asymmetric toward $CaMgSiO_4$). Consequently, we may further simplify our analysis by treating the $(Ca,Mg)MgSiO_4$ solution in terms of a one-constant (symmetric) formulation of the thermodynamic excess functions.

Following the notation of Thompson (1967), we have chosen the adjustable Margules parameter W_G to represent the excess molar Gibbs free energy:

$$\bar{G}_{ex} = N_1 N_2 W_G \tag{3}$$

when N_1 and N_2 here refer to mole fractions of the components $CaMgSiO_4$ and Mg_2SiO_4, respectively. For computational convenience, we have defined W_G as the average value of the asymmetric parameters (Thompson, 1967) W_{G1} and W_{G2}:

$$W_G \equiv \frac{W_{G1} + W_{G2}}{2} \tag{4}$$

For each observed pair of coexisting phases, N_{2A} and N_{2B} (A and B refer to the $CaMgSiO_4$-rich and Mg_2SiO_4-rich phases, respectively), values for W_{G1} and W_{G2}, and thus for W_G, were computed according to equations given on page 674–675 of Thompson and Waldbaum (1969).

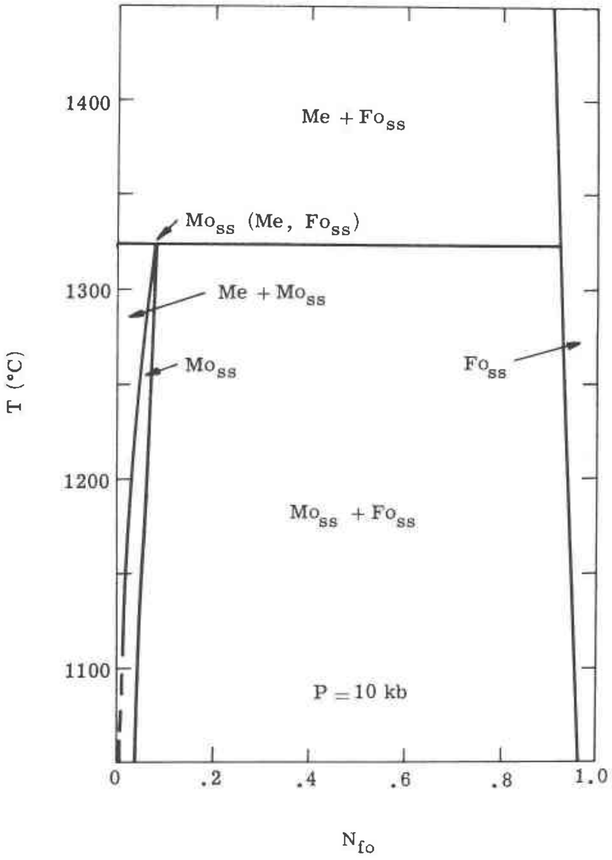

FIG. 3. Schematic temperature-composition diagram illustrating possible phase relations on the join $CaMgSiO_4$–Mg_2SiO_4 at 10 kbar. Abbreviations: Me, merwinite; Mo_{ss}, monticellite crystalline solution; Fo_{ss}, forsterite crystalline solution.

Since N_{2A} and N_{2B} are pressure and temperature dependent, it follows that the Margules parameter W_G is a function of both pressure and temperature. By deriving an equation of best fit for the complete set of polybaric, polythermal data, we thus obtain an expression which relates chemical composition to pressure and temperature for the monticellite-forsterite crystalline series. To determine an equation of best fit, least squares fits to various simple polynomial functions in T and P were investigated. The "estimated standard error" of Deming (p. 168, 1943), defined by

$$s_y = \left(\sum_{i=1}^{n} (y_i(\mathrm{obs}) - y_i(\mathrm{calc}))^2/(n-p)\right)^{1/2} \quad (5)$$

for the case of equally weighted data points, was used as a measure of the standard deviation of the dependent variable (here, W_G). In Equation (5), n represents the number of data points, p is the number of adjustable parameters in the fitted polynomial, and (n-p) gives the number of degrees of freedom. The parameter s_y satisfies the Gauss criterion for selection of the best equation that fits a given set of data (Thompson and Waldbaum, 1969). The standard errors of the polynomial coefficients, e_j, were computed from

$$e_i = s_y\,|c_{ii}|^{1/2} \quad (6)$$

where c_{jj} are diagonal terms of the inverse of the normal equations matrix (Deming, 1943).

Results of Numerical Analysis

Results of polybaric-polythermal least squares fits for the Margules parameter W_G are presented in Table 5. In evaluating these results, we are interested in (1) adopting the best representation of the data and also (2) keeping our equation as simple as possible. The best fit is obtained with an equation of the form:

$$W_G = \mathrm{A} + \mathrm{B}T + \mathrm{C}T^2 + \mathrm{D}P + \mathrm{E}PT \quad (7)$$

which reduces to a quadratic in T under isobaric conditions. This result apparently reflects the tendency for the two-phase region to widen at higher temperatures (Table 4), which results in solubility maxima in the delimiting boundary curves. The present data do not justify the adoption of a simpler (*i.e.*, linear in both T and P) expression.

Since

$$\bar{G}_{\mathrm{mix}} = RT\,(N_1 \ln N_1 + N_2 \ln N_2) + \bar{G}_{\mathrm{ex}} \quad (8)$$

we shall write for the molar Gibbs free energy of mixing:

$$\begin{aligned}\bar{G}_{\mathrm{mix}} &= RT\,(N_1 \ln N_1 + N_2 \ln N_2) + 20{,}338\\ &\pm 2355 - 13{,}560 \pm 3412(T/1000) + 3627\\ &\pm 1228(T/1000)^2 - 355.4 \pm 87.5P + 308.7\\ &\pm 65.4P(T/1000)N_1N_2,\ s_y = 297.4 \quad (9)\end{aligned}$$

Here R is the universal gas constant (1.98717 calories $^\circ\mathrm{K}^{-1}$ mole^{-1}), P is in kilobars, and T is in degrees Kelvin (the units of $\bar{G}_{\mathrm{mix}}$ thus are calories per mole). Equation (9) may be taken as an equation of state which describes the monticellite-forsterite binary crystalline solutions in the system $\mathrm{CaMgSiO_4}$-$\mathrm{Mg_2SiO_4}$.

In treating phase reactions in multicomponent systems, it is frequently convenient to have information concerning the activities of the various participating phases. Relative activities may be computed from the equations:

$$RT \ln a_1 = RT \ln N_1 + N_2^2 W_G \quad (10)$$

$$RT \ln a_2 = RT \ln N_2 + N_1^2 W_G \quad (11)$$

(Thompson, p. 349, 1967), where W_G is given by Equation (7) (coefficients in Table 5).

Calculated Temperature-Composition Sections

Points delimiting the boundary of the two-phase region may be obtained by resolving Equation (7) for N_{2A} and N_{2B} by an iterative procedure (Thompson and Waldbaum, 1969) or, alternatively, by direct calculation from Equations (10) and (11), utilizing the chemical potential equivalence condition for the

TABLE 5. Polybaric-Polythermal Least Squares Fits to W_G

A	B	C	D	E	F	s_y
--	5,943 ±225	--	205.3 ±53.6	--	--	1,487.5
12,052 ±383	-2,453 ±272	--	55.2 ±13.7	--	--	355.7
13,439 ±519	-3,476 ±376	--	-266.0 ±89.7	241.3 ±66.8	--	323.9
20,338 ±2,355	-13,560 ±3,412	3,627 ±1,228	-355.4 ±87.5	308.7 ±65.4	--	297.4
13,535 ±3,303	-3,571 ±4,817	123 ±1,737	2,277 ±760	-3,673 ±1,149	1,485 ±428	337.1

W_G = A + B (T/1000) + C $(T/1000)^2$ + DP + EP (T/1000) + FP $(T/1000)^2$

s_y = estimated standard error of dependent variable

units: W_G, cal/mole; T, °K; P, kb

isobaric-isothermal coexistence of the two phases expressed in terms of relative activities:

$$RT \ln a_{1A} = RT \ln a_{1B} \quad (12)$$

$$RT \ln a_{2A} = RT \ln a_{2B} \quad (13)$$

(Scatchard, 1940; Luth and Fenn, in preparation). Isobaric temperature-composition sections obtained by the latter method (procedure described in Luth and Fenn, in preparation) at 2 and at 10 kbar are shown as solid curves in Figure 2. Agreement between the calculated solvi and the experimental data is extremely good.

Of necessity, the calculated curves in Figure 2 represent a smoothing of the experimental data in a way that is internally consistent. This smoothing provides a basis for extrapolation to conditions of temperature and pressure beyond the range of experimental observation, but, in so doing, there is no guarantee that the calculated curves will continue to yield a close approximation of the solvi boundaries. The occurrence of polymorphic transitions or other phase reactions, such as the high pressure breakdown of monticellite suggested by the 10 kbar data, can only be verified by additional phase equilibrium data outside the P, T realm investigated in this study.

Discussion

The relative merits of the abridged Margules equation for binary solutions (as opposed to more sophisticated theoretical models, such as the "quasi-chemical" model) have been discussed by Thompson (1967), Thompson and Waldbaum (1969), Green (1970), and others. The adequacy of any particular thermodynamic model for a given application is determined by its success (or lack of success) in predicting measurable thermodynamic properties of that system. The data are not presently at hand with which to evaluate the success of Equation (9) for describing the mixing properties of monticellite-forsterite crystalline solutions in the system $CaMgSiO_4$-Mg_2SiO_4. (In the absence of direct measurements at the conditions of synthesis, it would be misleading to use the unit cell volumes from Table 3 as a basis for comparison with $\bar{V}_{mix}$ as implied by Equation (9).)

It should be noted that Equation (9) requires a negative volume of mixing at low temperature, but a positive volume of mixing at high temperature. The temperature of separation of these two regions is 890°C and is independent of pressure. In a similar sense, Equation (9) requires a negative excess entropy at high temperature and high pressure and a positive excess entropy at low T and low P. The two regions of P,T space are separated by the condition

$$W_s = 0 = -\left(\frac{\partial W_G}{\partial T}\right)_P \quad (14)$$

and the corresponding equation

$$T(°K) = 1869 - 0.04256P \text{ (bars)} \quad (15)$$

Petrologic Implications

The experimental results from this study place limits on the potential Ca content of naturally-occurring Mg-rich olivines. The maximum solubility of $CaMgSiO_4$ in Mg_2SiO_4 as a function of pressure and temperature, as calculated from Equation (9), is shown in Figure 4. The isocompositional curves shown in Figure 4 indicate the low-temperature stability limits of a given crystalline solution. At temperatures less than the values indicated by these curves, the composition shown would be a two-phase $Mo_{ss} + Fo_{ss}$ assemblage.

At temperatures below 800°C, less than one mole

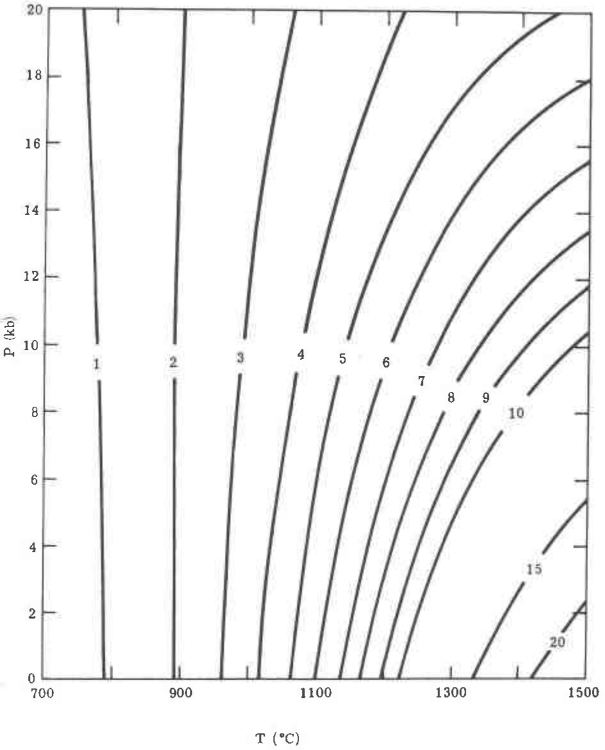

FIG. 4. Maximum solubility of $CaMgSiO_4$ in Mg_2SiO_4 as a function of pressure and temperature. Isocompositional curves (mole percent) calculated from Equation (9).

percent $CaMgSiO_4$ may be dissolved in forsterite. Consequently, olivines from metamorphic rocks, even those crystallizing in lime-rich rocks, such as occur during the metamorphism of impure dolomitic limestones, contain only trace amounts of calcium. At temperatures compatible with magmatic crystallization of Mg-rich olivine, it is theoretically possible to dissolve 5–10 mole percent $CaMgSiO_4$ (1.25–2.5 wt percent Ca) in forsterite. However, the compositions of most basic magmas are undersaturated with respect to monticellite, and the Ca content of igneous olivines is less than this maximum amount. Simkim and Smith (1970) published 251 partial analyses of natural igenous olivines. Their data indicate that Ca ranges from 0 to 1 wt percent. Without exception, analyses showing highest Ca content are either iron-rich olivines (where higher Ca contents might be anticipated because Ca $\leftrightarrows$ Fe substitution theoretically should be more extensive than Ca $\leftrightarrows$ Mg) or olivines from melilite-bearing rocks (*e.g.*, olivine-melilite nephelinite). Olivines from basalts, peridotites, and chemically similar rocks generally contain less than 0.25 wt percent Ca.

The data of Simkin and Smith (1970) are consistent with phase equilibrium data obtained for the system CaO-MgO-SiO_2 (Figure 5). In this system, forsterite coexisting with two pyroxene phases contains only 2 mole percent $CaMgSiO_4$ at 1350°C and 1 atm, and less than one mole percent $CaMgSiO_4$ at 1200°C throughout the pressure range 1-10 kbar (Warner, unpublished data). This represents significantly less solid solution than would be possible if the assemblage were saturated with $CaMgSiO_4$ (compare Fo'''_{ss} with Fo'_{ss} in Figure 5). Olivines from iron-poor basic and ultrabasic rocks should thus be noticeably impoverished in Ca, and this is borne out by the analyses given in Simkin and Smith (1970). However, forsterite coexisting with synthetic diopside and akermanite crystalline solutions (Fo''_{ss} in Figure 5) accomodates approximately 5 mole percent $CaMgSiO_4$ at 1200°C and 2 kbar (Warner, unpublished data). Hence, olivines from melilite-bearing igneous rocks might be expected to contain upwards of 1 wt percent Ca. Two out of four analyses of olivines from olivine-melilite nephelinites show greater than 1 wt percent Ca (Simkin and Smith, p. 311, 1970).

The effect of pressure is to decrease the solubility of $CaMgSiO_4$ in Mg_2SiO_4 (Figure 4). At temperatures above 1100°C, this becomes an appreciable factor, and might explain the inverse correlation of depth of crystallization with Ca content of olivine noted by Simkin and Smith (1970). Although extrapolation to *P,T* conditions beyond the data is admittedly hazardous, the curves shown in Figure 4 imply that, even for very calcic assemblages, forsterite cannot be an effective reservoir for calcium in the mantle.

From Equation (9) it may be inferred that metamorphic monticellites should be equally restricted in composition. In rare igneous parageneses, wherein monticellite characteristically occurs in reaction relation with early-formed Mg-rich olivine (*e.g.*, Bowen, 1922; Ukhanov, 1963), monticellite would be expected to dissolve 5–10 mole percent Mg_2SiO_4. The results from this study suggest that the upper stability limit of monticellite occurs at both higher temperature and higher pressure than indicated by Yoder (1968). The reaction $Mo_{ss} = Me + Fo_{ss}$ originates from an invariant equilibrium involving Mo_{ss}, Fo_{ss}, Me, Ak_{ss}, and Di_{ss} (Yoder, 1968; Warner,

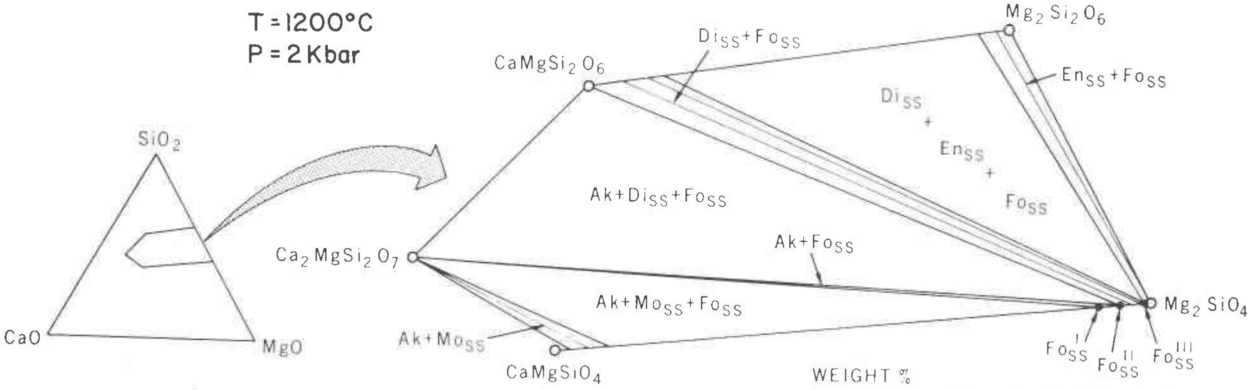

FIG. 5. Subsolidus phase relations for a portion of the system CaO-MgO-SiO_2 at 1200°C and 2 kbar. Solid circles indicate approximate compositions of isothermally, isobarically invariant forsterite crystalline solutions coexisting with Ak + Mo_{ss}(Fo'_{ss}), Ak + Di_{ss}(Fo''_{ss}), and Di_{ss} + En_{ss} (Fo'''_{ss}).

1971). Supplementary data bearing on this equilibrium corroborate the *P,T* coordinates given by Yoder (1968) for this invariant point (Warner, 1971). It is therefore probable that the *P,T* curve for the breakdown of monticellite is not significantly displaced from that given by Yoder (1968). The maximum depth in the earth to which monticellite is stable may thus be estimated at 35–40 km.

Appendix

Experimental Apparatus and Procedure

All experiments were performed either in an internally-heated pressure vessel, modified after Yoder (1950), and utilizing argon as the pressure medium, or in a quench furnace at atmospheric pressure.

Temperature in the quench furnace was measured with an unsheathed Pt/Pt-10 percent Rh thermocouple, with the reference junction maintained at the ice point. The melting point of diopside (1391.5°C) was used as a calibration standard, and reported temperatures are believed accurate to ±5°C. Samples consisted of unsealed platinum foil envelopes or sealed platinum capsules (cut from 2.0 mm O.D. tubing), and were suspended from a ceramic thermocouple support rod by means of thin platinum wire.

An inconel-sheathed Pt/Pt-10 percent Rh thermocouple was used to measure temperature in the internally-heated pressure vessel. Frequent calibrations were made against the known melting points of gold and sodium chloride (sodium sulfate was periodically used as a check). Reported temperatures are believed accurate to ±10°C for experiments at temperatures less than 1200°C, and to ±15°C for those in excess of 1200°C (where the thermocouple decay became a factor in experiments of more than several hours duration).

Argon pressure was generated via a two-stage Harwood intensifier. Pressure was measured by means of a manganin-cell pressure sensor by balancing the readout on a Carey-Foster bridge. Precision using this arrangement is estimated at ±250 psi; in general, because of minor pressure leaks, the standard error for reported pressures is about 3 percent of total run pressure.

Standard techniques of hydrothermal experimentation, as discussed by Roy and Tuttle (1956), were employed. Samples consisted of platinum or gold capsules, cut from 2.0 mm O.D. tubing, into which distilled, deionized water and anhydrous starting material were weighed prior to sealing. These were loaded in a molybdenum sample holder designed so that the capsules rested at the same depth as the tip of the sheathed thermocouple.

Starting materials used in this investigation were prepared as follows. "Fisher's Certified" $CaCO_3$ and "Baker's Analyzed" MgO were fired for 24 hours at 380° and 1300°C, respectively. High-purity silica glass (15 ppm phosphate precipitate), provided by Dr. O. F. Tuttle, was crushed, ground, and then heated for 2 hours. About ten grams each of the compositions $CaMgSiO_4$ and Mg_2SiO_4 were weighed out from the purified reagents and ground under acetone in an agate mortar in order to mix homogeneously. The compositions were then placed in clean platinum crucibles and individually fired at 1350°C for 24 hours. The process of grinding and subsequent firing was repeated through several cycles, but failed to result in complete crystallization. Compositions at 5 wt percent intervals along the join $CaMgSiO_4$–Mg_2SiO_4 were prepared as mechanical mixtures of the end-members. These were ground in an agate mortar under acetone until the average particle size was less than 20 microns (maximum grain sizes observed were approximately 50 microns in their greatest dimension).

After each experiment, the samples were examined with a petrographic microscope, using oil immersion grain mounts. For precision analysis, X-ray powder diffraction studies, utilizing a Nonius Guinier-deWolff focusing camera, were employed. Spinel (U.S. Bureau of Mines, Norris, Tennessee: a = 8.0833 Å at 25°C) was added to each sample as an internal standard. Exposures of approximately 20 hours duration were taken using Kodak single-coated blue-sensitive film with Cu$K\alpha$ radiation. The films were measured with a spectrum line measuring comparator (Grant Instrument Co.); reproducibility to ±0.002° 2θ was common on sharp peaks. Values reported for 2θ are believed accurate to ±0.01°.

Unit cell parameters of synthetic olivines were obtained through use of a least squares cell refinement computer program, developed by Evans *et al* (1963), and modified for use on an IBM 360/67 computer. Unit weights were assigned to all peaks, and the fixed index option of the program was used.

Acknowledgments

The results presented in this paper are based on a Ph.D. dissertation by Richard Warner submitted to the Department of Geology, Stanford University. The financial support of the National Science Foundation, both in the way of a graduate fellowship (RDW) and through NSF Grant GA 4164 (WCL) is most gratefully acknowledged. We wish to thank Mr. P. R. Gordon for his expert technical assistance, and Mr. P. M. Fenn for helping to develop the necessary computer programs for the data analysis. Important contributions to substance and presentation have arisen from discussions with Professor F. W. Dickson (Stanford University) and Dr. S. K. Saxena (then at NASA/Goddard Space Flight Center). This paper has benefited from critical review by John Grover.

References

BIGGAR, G. M., AND M. J. O'HARA (1969) Monticellite and forsterite crystalline solutions. *J. Amer. Ceram. Soc.* **52,** 249–252.

BIRLE, J. D., G. V. GIBBS, P. B. MOORE, AND J. V. SMITH (1968) Crystal structures of natural olivines. *Amer. Mineral.* **53,** 807–824.

BOWEN, N. L. (1922) Genetic features of alnoitic rocks at Isle Cadieux, Quebec. *Amer. J. Sci.,* 5th ser. **3,** 1–34.

DEMING, W. E. (1943) *Statistical Adjustment of Data.* John Wiley and Sons, New York. 261 pp.

EVANS, H. T., D. E. APPLEMAN, AND D. S. HANDWERKER (1963) The least square refinement of crystal unit cells with power diffraction data by an automatic computer indexing method. *Program, Annu. Meet. Amer. Crystallogr. Assoc.* pp. 42–43.

FERGUSON, J. B., AND H. E. MERWIN (1919) Ternary system CaO–MgO–SiO_2. *Amer. J. Sci.,* 4th ser. **48,** 81–123.

GREEN, E. J. (1970) Predictive thermodynamic models for mineral systems. I. Quasi-chemical analysis of the halite-sylvite subsolidus. *Amer. Mineral.* **55,** 1692–1713.

KUSHIRO, I., AND H. S. YODER, JR. (1964) Breakdown of monticellite and akermanite at high pressures. *Carnegie Inst. Washington Year Book,* **63,** 81–83.

ONKEN, H. (1965) Verfeinerung der Kristallstruktur von Monticellit. *Tschermak's Mineral. Petrogr. Mitt.* **10,** 34–44.

RICKER, R. W., AND E. F. OSBORN (1954) Additional phase equilibrium data for the system CaO–MgO–SiO_2. *J. Amer. Ceram. Soc.* **37,** 133–139.

ROY, R., AND O. F. TUTTLE (1956) Investigations under hydrothermal conditions. *Phys. Chem. Earth,* **1,** 138–180.

SAXENA, S. K. (1972) Retrieval of thermodynamic data from a study of intercrystalline and intra-crystalline ion-exchange equilibrium. *Amer. Mineral.* **57,** 1782–1800.

SCATCHARD, G. (1940) The calculation of the composition of phases in equilibrium. *J. Amer. Chem. Soc.* **62,** 2426–2429.

SHANNON, R. D., AND C. T. PREWITT (1969) Effective ionic radii in oxides and fluorides. *Acta Crystallogr.* **25,** 925–946.

SIMKIN, T., AND J. V. SMITH (1970) Minor-element distribution in olivine. *J. Geol.* **78,** 304–325.

THOMPSON, J. B., JR. (1967) Thermodynamic properties of simple solutions. In, *Researches in Geochemistry,* Vol. 2, Ed. P. H. Abelson. John Wiley and Sons, New York, pp. 340–361.

———, AND D. R. WALDBAUM (1969) Analysis of the two-phase region halite-sylvite in the system NaCl–KCl. *Geochim. Cosmochim. Acta,* **33,** 671–690.

UKHANOV, A. V. (1963) Olivine melilitite from the diamond-bearing diatremes on Anabar. *Akad. Nauk. SSSR Dokl., Earth Sci. Sec.* **153,** 176–178.

WARNER, R. D. (1971) *Experimental investigations in the system CaO–MgO–SiO_2–H_2O.* Ph.D. Thesis, Stanford University. 165 pp.

——— (1973) Liquidus relations in the system CaO-MgO-SiO_2-H_2O at 10 kb P_{H_2O} and their petrologic significance. *Amer. J. Sci.* (in press).

YANG, H. Y. (1973) New data on forsterite and monticellite solid solutions. *Amer. Mineral.* **58,** 343–345.

YODER, H. S., JR. (1950) High-low quartz inversion up to 10,000 bars. *Amer. Geophys. Union Trans.* **31,** 827–835.

——— (1968) Akermanite and related melilite-bearing assemblages. *Carnegie Inst. Washington Year Book,* **66,** 471–477.

Manuscript received, October 26, 1972; accepted for publication, June 21, 1973.